UNSUPERVISED LINE NETWORK EXTRACTION FROM REMOTELY SENSED IMAGES BY POLYLINE PROCESS

Caroline Lacoste [*], Xavier Descombes [*], Josiane Zerubia [*] and Nicolas Baghdadi [+]

[*] Ariana, joint research group CNRS/INRIA/UNSA
INRIA, 2004 route des Lucioles - BP 93
06902 Sophia Antipolis cedex - FRANCE
Email: firstname.lastname@inria.fr
Web: http://www-sop.inria.fr/ariana/

[+] BRGM, French Geological Survey
3, avenue Claude-Guillemin - BP 6009
45060 Orléans - FRANCE
Email: n.baghdadi@brgm.fr
Web: http://www.brgm.fr/

ABSTRACT

This article presents a new stochastic geometric model for unsupervised extraction of line network (roads, rivers,...) from remotely sensed images. The line network in the observed scene is modeled by a polyline process, named CAROLINE. The prior model incorporates the topological properties of the network considered through potentials on the polyline shape and interactions between polylines. Data properties are taken into account through a data term based on statistical tests. Optimization is realized by simulated annealing using a RJMCMC algorithm. Some experimental results are provided on aerial and satellite images.

1. INTRODUCTION

More than a half of the globe remains to be mapped. Consequently, many methods have been - and will be - developed in order to extract cartographic items for the production or the update of geographical data. In this context, we have been interested in extracting line networks (roads, rivers,...) from remotely sensed images. One possibility is to consider a semi-automatic approach where an operator gives some checking points [1–3] in order to initialize a road tracking algorithm. This approach can be extended to a fully-automatic one by using a previous detection obtained by a local optimization [4–6]. This type of technique, however, is strongly sensitive to the pre-detection.

In this paper, we present a fully-automatic technique for line network extraction which is not based on a combination of several stages of processing of the image. We model the line network in the image by a spatial process in a compact $F \subset \mathbb{R}^2$, that is a random set of objects whose number of objects located in F is a random finite variable. Such models, introduced in image processing in [7], provide the same type of stochastic properties as those of Markov random fields, while incorporating strong geometric constraints. In [8, 9], road extraction is performed using spatial processes whose objects are interacting line segments described by three random variables: their midpoint, their length, and their orientation. We extend this modeling to more complex objects, such as in [10] for cell recognition, where objects are variable resolution deformable templates. More exactly, our new model, called CARtographic Oriented LIne Network Extraction (CAROLINE), is a spatial process where objects are interacting polylines composed by an unknown number of segments. In comparison with [8, 9], the connection between segments is embedded into the object definition and thus extracted line networks should be more continuous; the road and river junctions are better modeled; and polylines can better fit sinuous line network than models based on segments.

The first author thanks the BRGM for partial funding and IGN (French Mapping Institute) for providing aerial data.

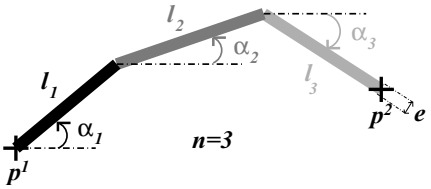

Figure 1: A typical object of the CAROLINE model.

The CAROLINE prior model is presented in Section 2. Data properties are taken into account in a data term, presented in Section 3. The optimization - described in Section 4 - is done via a simulated annealing. This algorithm is tested in Section 5 on remotely sensed images (aerial and satellite data).

2. PRIOR MODEL

2.1 Model for an unknown number of polylines

CAROLINE process is a random configuration of polylines, located in a compact set F of $\mathbb{R}^2$ corresponding to the observed scene, whose number N of polylines is unknown. Each polyline o is described by: its initial point $p^1 \in F$; its width $e \in [e_{min}, e_{max}]$; an unknown number $n \in \{1, \ldots, n_{max}\}$ of segments, which are described by their length $l_j \in [L_{min}, L_{max}]$ and their orientation $\alpha_j \in]-\pi, \pi]$. An example for $n = 3$ segments is given in Fig. 1.

We first define a reference process which is a completely random process. Under the reference process law, the polyline number N follows a Poisson law and polyline parameters, $\{p^1, e, n, \{l_j\}_{j=1..n}, \{\alpha_j\}_{j=1..n}\}$, are independently and uniformly distributed in their respective state space.

To introduce an *a priori* on polyline shapes and interactions between polylines, we then specify the CAROLINE prior process by a prior density h_p with respect to the reference process law. The expression of h_p is given in Section 2.3 after a presentation of the possible interactions between polylines in Section 2.2.

2.2 Polyline interactions

We consider two types of interaction.

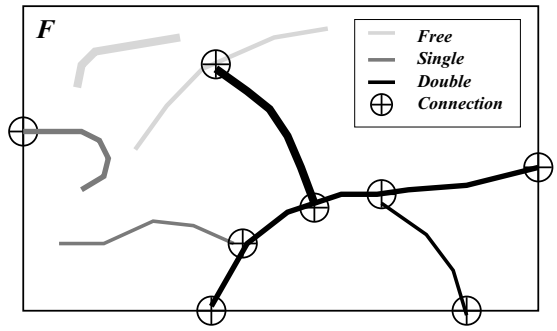

Figure 2: Polyline states with respect to connection.

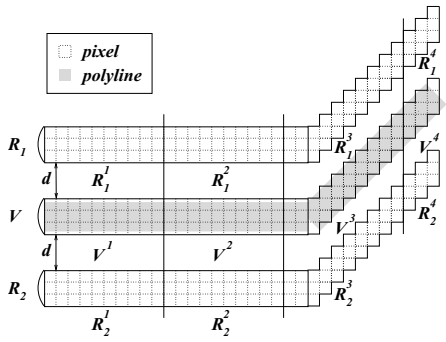

Figure 3: Pixel mask associated to a polyline.

The first one is based on a relation of proximity P between polylines. This interaction is forbidden in order to avoid too close polylines. When this interaction occurs for a given polyline configuration C, the density $h_p(C)$ is thus equal to zero.

The second interaction is based on the Euclidean distance between the endpoints p_o^1 and p_o^2 of a polyline o and another polyline or one edge of the compact F. If the distance $d(p_o^k, c)$ between p_o^k and c (polyline or edge) is lower than a threshold ε, o is said connected to c through p_o^k. Let $V_{C,F}(o)$ be the set of polylines and edges of C and F such that $d(p_o^1, c) < \varepsilon$ or $d(p_o^2, c) < \varepsilon$. A polyline o is said: free, if the set $V_{C,F}(o)$ is empty; single, if o is connected by only one of its endpoints; double, if o is connected by both of its endpoints. This is illustrated in Fig. 2.

2.3 CAROLINE prior density

The prior density h_p of a polyline configuration $C = \{o_1, \ldots, o_N\}$ can be written in Gibbsian form as follows:

$$h_p(C) = \begin{cases} 0 \text{ , if } \exists\, o_i \in C, o_j \in C / o_i \sim_P o_j \\ \frac{1}{Z} \exp - \sum_{i=1}^{N} \left[U_1(o_i) + U_2(o_i, V_{C,F}(o_i)) \right] \text{, if not} \end{cases} \quad (1)$$

where Z is an unknown normalizing constant, $o_i \sim_P o_j$ means that o_i and o_j verify the proximity relation P, U_1 is a potential based on the object shape and U_2 a potential based on the polyline connections.

The energy term U_1 associated to a polyline o composed of n segments is written as follows:

$$U_1(o) = \begin{cases} +\infty \text{ , if } o \text{ self-intersects} \\ U_{11}(n) + \sum_{j=1}^{n} U_{12}(l_j) + \sum_{j=1}^{n-1} U_{13}(\alpha_j, \alpha_{j+1}) \text{ , if not} \end{cases} \quad (2)$$

$$\text{with:} \quad \begin{aligned} U_{11}(n) &= \frac{M_n}{(n+1)^2} \\ U_{12}(l_j) &= M_l \frac{L_{max} - l_j}{L_{max} - L_{min}} \\ U_{13}(\alpha_j, \alpha_{j+1}) &= M_\alpha \left(0.5 - \cos(\alpha_{j+1} - \alpha_j)\right) \end{aligned}$$

where M_n, M_l and M_α are positive weights. U_{11} penalizes small n, U_{12} favors long segments and U_{13} favors small curvature. Moreover, self-intersection is forbidden by introducing a hard-core potential.

The energy term U_2 is written as follows:

$$U_2(o, V_{C,F}(o)) = U_{21}(o / V_{C,F}(o)) + \sum_{c \in V_{C,F}} U_{22}(o, c) \quad (3)$$

where U_{21} penalizes free and single segments by constant and positive potentials; U_{22} favors each connection between an endpoint p_o^k and a polyline, or an edge c by a negative potential which is based on a function measuring the quality of the connection. This function depends on the distance between p_o^k and c. The more distance decreases, the more the potential value decreases.

3. DATA TERM

We build a data term based on the following assumptions :

- H_1: The grey level variation between the network and the background is large;
- H_2: The local average of the grey level inside the network is homogeneous.

To verify that a polyline is well-fitted to the data, we consider a mask of pixels composed of the set of pixels V corresponding to the polyline in the image and two collinear regions R_1 and R_2, positioned at a distance d from V, corresponding to the nearby background. Each pixel mask is divided in sections of fixed number of pixels as shown in Fig. 3.

Firstly, the contrast hypothesis is checked for each section $M^i = \{V^i, R_1^i, R_2^i\}$. The test value t_c^i associated to M^i is the minimum of the two Student t-test values between the internal section V^i and the two external sections R_1^i and R_2^i. Then, we perform a thresholding of t_c^i between t_1 and t_2 followed by a linear transformation from $[t_1, t_2]$ to $[-1, 1]$ in order to obtain a potential, $U_c(i)$, measuring H_1 for the section M^i.

Secondly, the homogeneity hypothesis H_2 is checked by computing the Student t-test values t_h^i between successive internal sections V^i and V^{i+1}. Then, we perform a thresholding of t_h^i between 1 and t_3 followed by a linear transformation from $[1, t_3]$ to $[-1, 1]$ in order to obtain a potential, $U_h(i, i+1)$, measuring H_2 for $\{V^i, V^{i+1}\}$.

Finally, the data potential associated to a polyline is the following:

$$U_d(o) = p_c \sum_{i=1}^{I} U_c(i) + p_h \sum_{i=1}^{I-1} U_h(i, i+1) \quad (4)$$

where I is the number of sections of the pixel mask associated to o, p_c and p_h are positive weights respectively associated to the contrast potential U_c and the homogeneity potential U_h. The total energy for a given configuration C is the sum of data potential of each polyline belonging to C. The data term is thus given by:

$$h_d(C) \propto \exp\left(-\sum_{o_i \in C} U_d(o_i)\right) \quad (5)$$

where U_d is given by equation (4).

4. OPTIMIZATION

To extract the line network from an image, we aim to find a configuration of polylines which maximizes the unnormalized process density f given by:

$$f(C) \propto h_p(C)\, h_d(C) \quad (6)$$

where h_p and h_d are respectively given by equation (1) and equation (5). This is a non convex problem for which a direct optimization is not possible given the large size of the state space that is $\cup_{N=0}^{\infty} \Omega_N$ where Ω_N is the set of configurations of N polylines. We propose to estimate this maximum by a simulated annealing, which consists in successive simulations of the process distribution π_T specified by the density $f^{1/T}$, with T gradually dropping to 0. A proof of convergence is given in [11] when the decrease of temperature T is logarithmic. In practice, temperature decreases geometrically in order to reduce the computing time.

The algorithm chosen to simulate the unnormalized measure π_T is a RJMCMC algorithm. It consists of simulating a discrete Markov Chain of invariant measure π_T which performs small jumps between the spaces Ω_i [12, 13]. This iterative algorithm does not depend on the initial state. At each step, a transition from the current state to a new state is proposed according to a proposition kernel which is composed of several sub-kernels, each corresponding to a reversible move ("birth-and-death", symmetrical transformation, etc.). The transition is accepted with a probability given by Green's ratio, which is computed so that the detailed balance condition is verified [13].

Although it is sufficient to define uniform birth-and-death [12] in order to simulate spatial processes, it is important to define relevant moves in order to speed up the convergence of the Markov chain. In addition to a uniform "birth-and-death", we have thus defined a "birth-and-death" of polylines containing only one segment based on data (off-line computation of data term for small pixel masks) in order to propose segments correctly positioned. We also propose small perturbations very useful when a polyline is already well positioned: "dilation"of a polyline; "add-and-remove" a segment at the end or the beginning of a polyline; "move" a point of a polyline (an endpoint or a point between two segments); "split-and-merge" of segment. Moreover, we use a "split-and-merge" of polyline which is very relevant when two or more polylines are positioned on the same section of the real line network. All these moves are illustrated in Fig. 4.

5. RESULTS

This section provides results of the algorithm described in Section 4 on three remotely sensed images, with an initialization by the empty configuration.

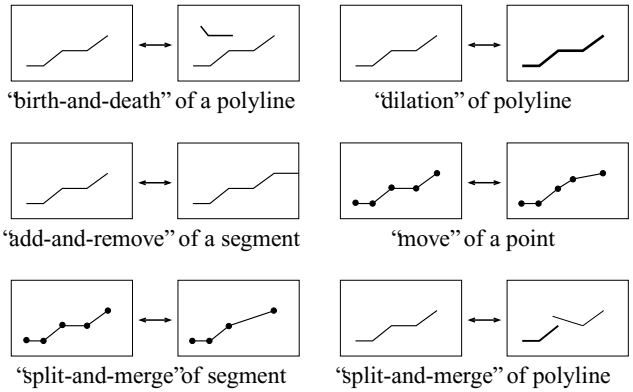

Figure 4: Reversible moves.

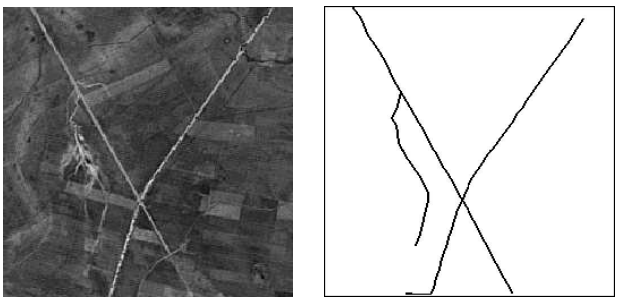

Figure 5: Road extraction from a satellite image (256×256 pixels).

The first image - see Fig. 5 - is a satellite image (SPOT Panchro, resolution: 10 m), where the sought-after cartographic item is the road network. The extraction algorithm provides a smooth and continuous line network with few omissions and no over detection. It extracts quite well not only the main roads, but also one dirt track which is not as rectilinear and clearly contrasted with respect to the background as the main roads.

The second image - see Fig. 6 - is a hight resolution (0.5 m) aerial image provided by French Mapping Institute (IGN), where the sought-after cartographic item is the road network. The task is not straightforward here, due to "geometrical noise" (for instance, trees near roads). Nearly all the roads have been detected. There is only one overdetection (near a house) and this overdetection is coherent with our *a priori* knowledge on road network topology as it is between two roads of the same orientation. The detection of junctions between roads is well done. Only two small breaks are due to the presence of trees between two polylines of different width. Polylines of varying width should be considered in the near future.

The last image - see Fig. 7 - is a satellite image (SPOT XS2, resolution: 20 meters) of Guinea provided by the French Geological Survey (BRGM), where the sought-after cartographic item is the hydrographic network. The latter is spotted by the presence of trees near rivers, and is named riverine forest. The extraction algorithm provides a continuous line network with no omission and just a few overdetections. Moreover, the line network extracted is very close to

data

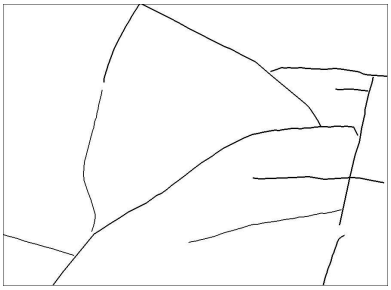

extracted network

Figure 6: Road extraction from an aerial image (892×652 pixels).

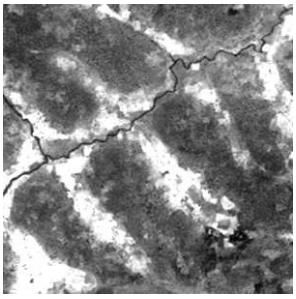

data

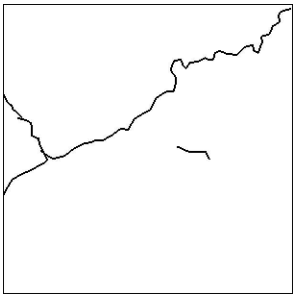

extracted network

Figure 7: River extraction from a satellite image (300×300 pixels).

the real one despite of the large local curvature of this network.

These results show that the polyline process CAROLINE is adapted to the extraction of line network. In particular, the detection of sinuous networks is more accurate and the road and river junctions are better detected than with the previous segment processes (see [14] for more details).

6. CONCLUSION

We have proposed in this paper a relevant method to perform line network extraction from satellite and aerial images. This is a fully automatic method without any initialization. Indeed, the use of a simulated annealing using a RJMCMC algorithm for the optimization allow us to initialize the algorithm with the empty configuration. The prior model leads to continuous extracted line networks with few omissions and overdetections. Results on remotely sensed images have shown that the polyline process CAROLINE is fitted to the extraction of sinuous networks and models correctly the road and river junctions thanks to the definition of a polyline connection. Moreover, the data term seems to perform well for different types of images. We will focus in the near future on the definition of an inhomogeneous reference process based on data that would be better adapted to our problem. Indeed, it would allow to accept more correctly positioned segment at the beginning of the algorithm. Moreover, the proposed stochastic modeling allows us to consider working in a frame of data fusion in order to benefit from the contribution of several sources (for instance, multi-sensor or multi-temporal data).

REFERENCES

[1] D. Geman and B. Jedynak, "An active testing model for tracking roads in satellite images," *IEEE Trans. on PAMI*, vol. 18, pp. 1–14, 1996.

[2] N. Merlet and J. Zerubia, "New prospects in line detection by dynamic programming," *IEEE Trans. on PAMI*, vol. 18, no. 4, pp. 426–431, 1996.

[3] W. M. Neuenschwander, P. Fua, L. Iverson, G. Székely, and O. Kubler, "Ziplock snakes," *International Journal of Computer Vision*, vol. 25, no. 3, pp. 191–201, 1997.

[4] M. Barzohar and D. B. Cooper, "Automatic finding of main roads in aerial images by using geometric-stochastic models and estimation," *IEEE Trans. on PAMI*, vol. 18 - 2, pp. 707–721, 1996.

[5] A. Zlotnick and P. Carnine, "Finding road seeds in aerial images," *Computer Vision, Graphics, and Image Processing*, vol. 57, pp. 243–260, 1993.

[6] F. Tupin, H. Maitre, J-F. Mangin, J-M. Nicolas, and E. Pechersky, "Detection of linear features in SAR images: Application to road network extraction," *IEEE Trans. on Geoscience and Remote Sensing*, vol. 36, no. 2, pp. 434–453, 1998.

[7] A. Baddeley and M. N. M. van Lieshout, "Stochastic geometry models in high-level vision.," in *Statistics and Images*, K.V. Mardia, Ed., vol. 1, pp. 233–258. Abingdon: Carfax, 1993.

[8] R. Stoica, X. Descombes, and J. Zerubia, "A Gibbs point process for road extraction in remotely sensed images," To appear in International Journal of Computer Vision.

[9] C. Lacoste, X. Descombes, and J. Zerubia, "Road network extraction in remote sensing by a Markov object process," in *ICIP*, Barcelona, Spain, Sept. 2003.

[10] H. Rue and M. Hurn, "Bayesian object identification," *Biometrika*, vol. 3, pp. 649–660, 1999.

[11] M.N.M. van Lieshout, "Stochastic annealing for nearest-neighbour point processes with application to object recognition," Research Report BS-R9306, CWI, The Netherlands, 1993.

[12] C. J. Geyer and J. Møller, "Simulation and likelihood inference for spatial point process," *Scandinavian Journal of Statistics, Series B*, vol. 21, pp. 359–373, 1994.

[13] P.J. Green, "Reversible jump Markov chain Monte-Carlo computation and Bayesian model determination," *Biometrika*, vol. 57, pp. 97–109, 1995.

[14] C. Lacoste, X. Descombes, and J. Zerubia, "A comparative study of point processes for line network extraction in remote sensing," Research report INRIA No. 4516, 2002.